

SUPPLEMENT MATERIAL

**Effect of early particulate air pollution exposure on obesity in mice: Role of p47<sup>phox</sup>**

Xiaohua Xu<sup>1</sup>, Zubin Yavar<sup>1</sup>, Matt Verdin<sup>1</sup>, Zhekang Ying<sup>2</sup>, Georgeta Mihai<sup>2</sup>, Thomas Kampfrath<sup>2</sup>, Aixia Wang<sup>2</sup>, Mianhua Zhong<sup>4</sup>, Morton Lippmann<sup>4</sup>, Lung-Chi Chen<sup>4</sup>, Sanjay Rajagopalan<sup>2,3</sup>, Qinghua Sun<sup>1,2,5</sup>

<sup>1</sup>Division of Environmental Health Sciences  
College of Public Health  
The Ohio State University  
Columbus, Ohio, USA

<sup>2</sup>Davis Heart and Lung Research Institute,  
The Ohio State University  
Columbus, Ohio, USA

<sup>3</sup>Division of Cardiovascular Medicine  
Department of Internal Medicine  
The Ohio State University  
Columbus, Ohio, USA

<sup>4</sup>Department of Environmental Medicine  
New York University School of Medicine  
Tuxedo, New York, USA

**Corresponding author:**

Qinghua Sun, M.D., Ph.D.  
Division of Environmental Health Sciences  
Biomedical Research Tower Room 396  
460 W 12th Avenue  
Columbus, OH 43210, USA  
Phone: (614) 247-1560  
Fax: (614) 688-4233  
E-mail: [sun.224@osu.edu](mailto:sun.224@osu.edu)

Online Supplemental Material includes:  
Materials and Methods  
Tables and Legends (Supplemental Tables I-II)  
Figures and Legends (Supplemental Figures I-IV)

## **Materials and Methods**

### **Mice**

We used male 3-week-old C57BL/6 mice and p47<sup>phox</sup><sup>-/-</sup> mice (both from Jackson Laboratories, Bar Harbor, MA). The protocol and the use of animals were approved by and in accordance with the Ohio State University (OSU) Animal Care and Use Committee.

### **Diet and PM<sub>2.5</sub> Exposure**

C57BL/6 and p47<sup>phox</sup><sup>-/-</sup> mice (32 mice each) were fed with either ND (Teklad 7012, 13% calories from fat, Harlan Teklad, TD 88137, Harlan, Indianapolis, IN; n = 16) or HFD (Teklad TD88137, 42% calories from fat, Harlan Teklad, n = 16) beginning at 3 weeks of age. The PM<sub>2.5</sub> exposure protocol was described previously.<sup>1-3</sup> Briefly, animals were exposed to PM<sub>2.5</sub> at nominal 10× ambient concentrations 6 hours/day, 5 days/week for about 10 weeks in a mobile trailer exposure system “Ohio Air Pollution Exposure System for Interrogation of Systemic Effects (OASIS) 1” that is located at the OSU Animal Facility in Columbus, OH. The mice in the FA group (n = 16) were exposed to an identical protocol with the exception that a High Efficiency Particulate Air filter (HEPA) was positioned in the inlet valve to the exposure system to remove all of the PM<sub>2.5</sub> from that air stream, as detailed previously.<sup>1,4</sup> The ambient PM<sub>2.5</sub> concentrations in Columbus were monitored using an oscillating microbalance (Tapered-Element Oscillating Microbalance, Model 1400). For the concentrated ambient PM<sub>2.5</sub> in the exposure chambers, samples were collected on Teflon filters (Gelman Teflo, 37 mm, 2 µm pore) and weighed before and after sampling in a temperature and humidity-controlled

weighing room. The weight gains were used to calculate the exposure concentrations the mice were exposed.<sup>1,2</sup>

### **Energy-Dispersive X-Ray Fluorescence (ED-XRF)**

All PM samples for gravimetric and elemental analyses were collected on filters. Filter masses were measured on a microbalance (model MT5, Mettler-Toledo Inc., Highstown, NJ). Analyses for 35 elements followed by nondestructive XRF (model EX-6600-AF, Jordan Valley) using five secondary fluorescers (Si, Ti, Fe, Ge, and Mo) and spectral software XRF2000v3.1 (U.S. EPA and ManTech Environmental Technology, Inc.) as described elsewhere.<sup>5</sup>

### **Measurements of Blood Glucose Homeostasis and Insulin**

Before and after the exposure to FA or PM<sub>2.5</sub>, the mice were fasted overnight and dextrose (2 mg/g body weight) was injected intraperitoneally. Blood glucose measurement was conducted with an Elite Glucometer (Bayer) at baseline, and 30, 60, 90, and 120 minutes after the dextrose injection. Insulin levels were determined using an Ultra Sensitive Mouse Insulin ELISA Kit (Crystal Chem Inc., Downers Grove, IL). Homeostasis model assessment (HOMA) indices were calculated based on 1 mg of insulin as equivalent to 24 IU, using the formula  $HOMA = [fasting\ insulin\ concentration\ (ng/ml) \times 24 \times fasting\ glucose\ concentration\ (mg/dl)]/405$ .<sup>2</sup>

### **Magnetic Resonance Imaging (MRI)**

Abdominal fat mass was performed by *in vivo* MRI, as described previously.<sup>2</sup> Briefly, a Bruker 11.7T NMR system operating at a proton frequency of 500 MHz with a gradient strength of 300 gauss per centimeter was used. Mice were anesthetized with isoflurane (1.5-2.0%) and placed in a 30 mm birdcage coil. A coronal spin-echo localizing sequence was used to identify both kidneys. Thirty contiguous, 1-mm thick axial slices spanning from the superior pole of the uppermost kidney to the caudal aspect of the mouse were obtained using a spin-echo sequence with a 256×256 matrix size (pixel size, 117×117×1,000  $\mu\text{m}^3$ ). Data analysis was performed by Image J software downloaded from the NIH website (Image J, <http://rsb.info.nih.gov/ij/>). Using the T1-weighted images, total abdominal volume, total adipose tissue, subcutaneous adipose tissue, and visceral adipose tissue were calculated as follows: the images were converted into two intensities, one corresponding to the adipose regions and the other corresponding to the remaining tissue. From these binary images, total adipose volume is equal to the volume of the intensity corresponding to the adipose region and total abdominal volume is equal to the volume of both intensities combined. The subcutaneous adipose tissue was calculated by subtracting the visceral adipose tissue volume from the total adipose tissue volume.

### **Cell Migration Assays in Adipose Conditioned Media**

Cell migration was assayed using a modified Boyden chamber consisting of a 48-well microchamber (Neuro Probe, Gaithersburg, MD). Briefly, 10 mg of adipose tissue was incubated in 500  $\mu\text{l}$  of serum-free RPMI 1640 for 16 hours. After centrifugation, 26  $\mu\text{l}$  of the conditioned media was added to the lower wells, and an 8- $\mu\text{m}$  pore-size

polyvinylpyrrolidone-free polycarbonate membrane (Neuro Probe, Gaithersburg, MD) was placed between the lower wells and upper wells. THP-1 monocyte cells (ATCC #TIB-202) were suspended in culture medium at  $1 \times 10^6$  cells/ml, and 50  $\mu$ l aliquot of the cell suspension was then placed into the upper wells. The chamber was incubated for 4 hours at 37°C in a humidified incubator with 5% CO<sub>2</sub>. After incubation, the cells adherent to the upper surface of the membrane were removed by scraping with a rubber blade. The cells that had migrated through the membrane and were adherent to the underside of the membrane were fixed and stained with Hema-3 system (Fisher Scientific, Pittsburgh, PA), mounted, and the cell migration was quantified by counting under light microscope. The results are presented as migrated cell number/five high power fields (HPF) that were chosen randomly.

#### **NADPH Oxidase Derived Superoxide (O<sub>2</sub><sup>•-</sup>) Measurements**

NADPH oxidase activity in visceral and subcutaneous fat tissues was measured using lucigenin chemiluminescence to exogenously added NADPH, as described previously.<sup>6</sup> Briefly, tissues were placed in a modified Kreps-Hepes buffer (pH =7.4; initially gassed with 95% O<sub>2</sub>, and 5% CO<sub>2</sub>) and equilibrated for 30 min at 37°C. Scintillation vials containing 300  $\mu$ l of Krebs-Hepes buffer with 5  $\mu$ M Lucigenin were placed into an EG&G Berthold luminometer (Berthold Australia Pty Ltd, Australia). After a dark adaptation, background counts were recorded and tissues were added to the vial. Scintillation counts were then recorded every 2 min at 30-s intervals. After baseline measurements for 5 min, NADPH at 100 $\mu$ M was added to each vial and scintillation

counts were recorded every 30 s for 10 min. Measurements were then adjusted for tissue weight. Values were reported after subtracting respective background counts.

### **Intravital Microscopy**

Mice were anesthetized intraperitoneally by a mixture of ketamine (100 mg/kg) and xylazine (20 mg/kg). Ten million murine RAW 264.7 cells (ATCC, Manassas, VA) labeled with CFSE using CellTrace™ CFSE Proliferation Kit (Invitrogen, Carlsbad, CA) were retroorbitally injected, and cremaster muscle were exteriorized, mounted on a Plexiglas platform, and superfused with pre-warmed Ringer's lactate (37°C). The number of rolling and adherent cells in cremasteric muscle was determined with a 40×/0.80-W water-immersed objective using a Nikon Eclipse FN1 microscope (Nikon, Tokyo, Japan) in a 100-μm vessel length per 30 seconds per image field ( $1.57 \times 10^5 \mu\text{m}^2$ ), and the data presented were averaged from 10 vessels per mouse. Cells that remained stationary for at least 5 seconds were considered “adherent” cells.<sup>2</sup> Metamorph software (version 7.1.2.0, Metamorph, Downingtown, PA) was used for analysis of events.

### **Measurement of Blood Inflammatory Biomarkers**

Mice were fasted overnight prior to all blood collection and sacrifice. Blood was collected in anticoagulant, spun, and plasma stored at -70°C for the analysis of cytokine and chemokine biomarkers including interferon gamma (IFN-γ), monocyte chemoattractant protein (MCP)-1, regulated on activation normal T-cell expressed and secreted (RANTES), and tumor necrosis factor α (TNF-α) by a quantitative ELISA assay (Pierce Biotechnology, Woburn, MA).

### **Myograph Experiments**

Thoracic aortic rings (2 mm each) from the mice were mounted in individual organ chambers that were filled with physiological salt solution, as described previously.<sup>1,2</sup> The rings were subjected to graded doses of vasoconstrictor phenylephrine (PE,  $10^{-10}$  to  $10^{-5}$  mol/L). After a stable contraction plateau was reached with PE, which was about 50% of peak tension generated with 120 mmol/L of KCl, the rings were exposed to endothelium-dependent vasodilator Ach ( $10^{-10}$  to  $10^{-5}$  mol/L), or insulin ( $10^{-5}$  to  $10^{-2}$  mol/L, Novolin<sup>®</sup>, Novo Nordisk Inc, Princeton, NJ).

### **Histological Analysis**

Tissues were fixed in paraffin and cut into 10 sections (5  $\mu$ m thick) separated by 200  $\mu$ m. Sections were stained with H&E and visualized using a microscope. To examine the size of adipocytes in visceral fat, the major axis of each adipocyte was measured.<sup>2</sup>

### **Immunohistochemical Staining**

Deparaffinized sections (5  $\mu$ m) were subjected to heat-induced antigen retrieval by incubation in Retrieve-all-1 unmasking solution (Signet Labs, Dedham, MA) for 15 minutes at 95°C, cooled down to room temperature, and washed with PBS. The slides were dipped in 0.3% H<sub>2</sub>O<sub>2</sub>/methanol for 10 min to quench the endogenous peroxidase. After rinsing in phosphate buffered saline (PBS), the sections were incubated in 1% BSA/PBS for 10 minutes, followed by overnight incubation with rat anti-mouse F4/80 (AbD Serotec, Raleigh, NC) at 4°C. Then the slides were rinsed and incubated at room

temperature for 2 hours with appropriate horseradish peroxidase (HRP)-conjugated secondary antibodies. After the PBS rinsing, the stain was developed using Fast 3,3'-diaminobenzidine tablet sets (D4293; Sigma). The sections were then counterstained with hematoxylin and examined by light microscopy. All measurements were conducted in a double-blinded manner by two independent investigators.

### **Real-Time Polymerase Chain Reaction (RT-PCR)**

Visceral adipose tissues from the mice were excised, minced, and digested with collagenase type II, and the SVF isolated as described previously<sup>2</sup>. RNA was isolated using TRIzol Reagent (Invitrogen, Carlsbad, CA) according to the manufacturer's instructions. Total RNA was then converted into cDNA using the High Capacity cDNA Reverse Transcription Kit (Applied biosystems, Foster City, CA). The quantification of gene expression was determined by RT-PCR. All reactions were performed under the same conditions: 50°C for 2 minutes, 95°C for 10 minutes, 40 cycles of 95°C for 15 seconds, and 60°C for 1 minute. The primer sequences were described previously.<sup>2</sup>

### **Immunoprecipitation of p47<sup>phox</sup> and Western Blot**

Epididymal fat tissues were homogenized and the cleared supernatant was incubated overnight with anti-p47<sup>phox</sup> (1:100), and the protein was immunoprecipitated with protein G agarose (Pierce), washed 3 times in lysis buffer, and denatured in Laemmli sample buffer. The samples were subjected to sodium dodecyl sulfate-polyacrylamide gel (SDS-PAGE) in 10% polyacrylamide gel, and then transferred to PVDF membranes (Bio-Rad, Hercules, CA). For detection of phosphorylated protein, membranes were incubated with



anti-phosphoserine antibody (Abcam, Cambridge, MA) overnight at 4°C. Membranes were incubated with primary antibodies overnight at 4°C. For detection of p47<sup>phox</sup>, the membrane was stripped and incubated with rabbit anti-p47<sup>phox</sup> monoclonal antibody (Santa Cruz Biotechnology, Inc., Santa Cruz, CA) overnight. Membranes were then washed and incubated with horseradish peroxidase-conjugated secondary antibodies. The membranes were detected with enhanced chemiluminescence (Super Signal West Pico; Thermo Scientific, Rockford, IL) followed by exposure to X-ray film. The protein bands on the X-ray film were scanned, and band density was calculated by Quantity One software (Bio-Rad).

### **Statistical Analysis**

Data are expressed as mean  $\pm$  s.e. unless otherwise indicated. For responses measured repeatedly at different time points or dose levels, a series of 2-sample independent Student's *t* test were used to detect the significant differences between 2 treatment groups at every time point and dose level with the Bonferroni correction for multiple comparison adjustment. Comparisons of other continuous variables were conducted with an independent 2-sample Student *t* test, with values of  $P < 0.05$  considered significant.

## References

1. Sun Q, Wang A, Jin X, Natanzon A, Duquaine D, Brook RD, Aguinaldo JG, Fayad ZA, Fuster V, Lippmann M, Chen LC, Rajagopalan S. Long-term air pollution exposure and acceleration of atherosclerosis and vascular inflammation in an animal model. *Jama*. 2005;294:3003-3010.
2. Sun Q, Yue P, Deiuliis JA, Lumeng CN, Kampfrath T, Mikolaj MB, Cai Y, Ostrowski MC, Lu B, Parthasarathy S, Brook RD, Moffatt-Bruce SD, Chen LC, Rajagopalan S. Ambient air pollution exaggerates adipose inflammation and insulin resistance in a mouse model of diet-induced obesity. *Circulation*. 2009;119:538-546.
3. Chen LC, Nadziejko C. Effects of subchronic exposures to concentrated ambient particles (CAPs) in mice. V. CAPs exacerbate aortic plaque development in hyperlipidemic mice. *Inhal Toxicol*. 2005;17:217-224.
4. Maciejczyk P, Zhong M, Li Q, Xiong J, Nadziejko C, Chen LC. Effects of subchronic exposures to concentrated ambient particles (CAPs) in mice. II. The design of a CAPs exposure system for biometric telemetry monitoring. *Inhal Toxicol*. 2005;17:189-197.
5. Maciejczyk P, Chen LC. Effects of subchronic exposures to concentrated ambient particles (CAPs) in mice. VIII. Source-related daily variations in *in vitro* responses to CAPs. *Inhal Toxicol*. 2005;17:243-253.
6. Ying Z, Kampfrath T, Thurston G, Farrar B, Lippmann M, Wang A, Sun Q, Chen LC, Rajagopalan S. Ambient particulates alter vascular function through induction of reactive oxygen and nitrogen species. *Toxicol Sci*. 2009;111:80-88.

**Supplemental Table I.** Elemental concentrations of PM<sub>2.5</sub> particle during the exposure

	Mean	s.d.
S	5768.0	3061.0
Si	1312.0	878.0
Ca	597.0	359.9
Fe	565.9	380.8
Al	541.1	317.2
Na	341.7	203.2
K	279.4	156.4
Mg	225.9	174.1
Zn	94.8	73.9
Ti	38.2	26.5
P	36.4	49.7
Pb	25.5	7.3
Cl	25.3	40.3
Te	21.0	27.0
Sn	20.2	14.3
Br	18.5	10.1
Ba	18.1	16.3
Cu	17.6	10.4
In	17.6	22.1
Mn	16.2	10.2
Sb	12.4	13.5
Se	8.2	4.3
Cd	4.7	6.0
Ni	4.4	1.6
Cr	3.7	2.3
Sr	3.3	2.0
Cs	2.1	2.0
V	1.8	2.4
As	0.9	1.6
Rb	0.9	0.8
Ge	0.4	0.6
Ga	0.3	0.8
Co	0.2	0.3

Note: unit, ng/m<sup>3</sup>. s.d., standard deviation.

**Supplemental Table II.** Body weight of C57BL/6 and p47<sup>phox-/-</sup> mice before (baseline) and after 10-week exposure to PM<sub>2.5</sub> or FA

	C57BL/6 mice		p47 <sup>phox-/-</sup> mice	
	before	after	before	after
FA-ND	9.0 ± 0.3	24.7 ± 0.7	9.1 ± 0.4	22.3 ± 0.4
PM <sub>2.5</sub> -ND	8.9 ± 0.3	23.5 ± 0.5	9.0 ± 0.4	22.2 ± 0.5
FA-HFD	8.8 ± 0.2	33.4 ± 1.4 <sup>**</sup>	8.7 ± 0.2	31.1 ± 1.6 <sup>**</sup>
PM <sub>2.5</sub> -HFD	9.1 ± 0.2	32.4 ± 0.7 <sup>‡</sup>	8.7 ± 0.1	31.7 ± 0.7 <sup>‡</sup>

<sup>\*\*</sup>*P*<0.001 vs. corresponding FA-ND; <sup>‡</sup>*P*<0.001 vs. corresponding PM<sub>2.5</sub>-ND.

## Figure legends

**Supplemental Figure I.** Results of intraperitoneal glucose tolerance test (IPGTT) and abdominal fat mass before the exposure (baseline), and representative T1-weighted spin echo images of adipose tissues by magnetic resonance imaging (MRI) after exposure to PM<sub>2.5</sub> or FA in the mice fed normal chow diet (ND) or high-fat diet (HFD) in C57BL/6 (a-c) and p47<sup>phox</sup><sup>-/-</sup> (d-f) mice. n=8 in each group.

**Supplemental Figure II.** Adipocyte area and frequency distribution for the visceral fat (a-c) and subcutaneous fat (d-f) from the C57BL/6 mice exposed to PM<sub>2.5</sub> or FA (n=8). Adipocyte-size histograms show increased adipocyte hypertrophy in PM<sub>2.5</sub>-exposed mice. Areas were calculated from 90 adipocytes from each of 5 mice in each group. (a, d) Frequency of adipocytes of visceral fat from normal diet groups; (b, e) Frequency of adipocytes of visceral fat from high fat diet groups; (c, f) Box plot of adipocyte size. The box represents the upper and lower quartiles. The whiskers show the 5<sup>th</sup> or 95<sup>th</sup> percentile. The line in the box represents the median. The + signs in (c) and (f) represent the mean.

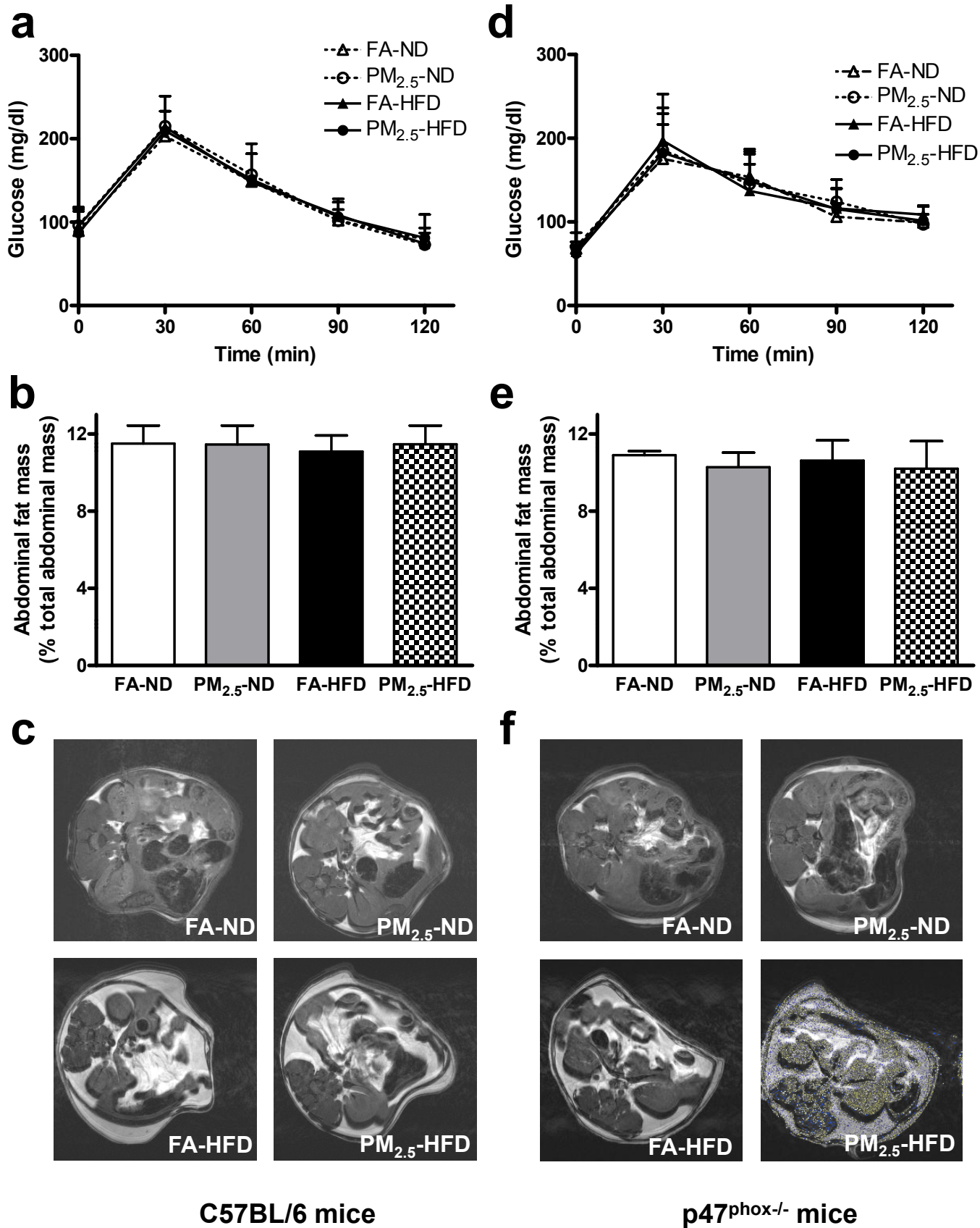
**Supplemental Figure III.** Adipocyte area and frequency distribution for the visceral fat (a-c) and subcutaneous fat (d-f) from the p47<sup>phox</sup><sup>-/-</sup> mice exposed to PM<sub>2.5</sub> or FA (n=8). Adipocyte-size histograms show increased adipocyte hypertrophy in PM<sub>2.5</sub>-exposed mice. Areas were calculated from 90 adipocytes from each of 5 mice in each group. (a, d) Frequency of adipocytes of visceral fat from normal diet groups; (b, e) Frequency of adipocytes of visceral fat from high fat diet groups; (c, f) Box plot of adipocyte size. The

box represents the upper and lower quartiles. The whiskers show the 5<sup>th</sup> or 95<sup>th</sup> percentile. The line in the box represents the median. The + signs in (c) and (f) represent the mean.

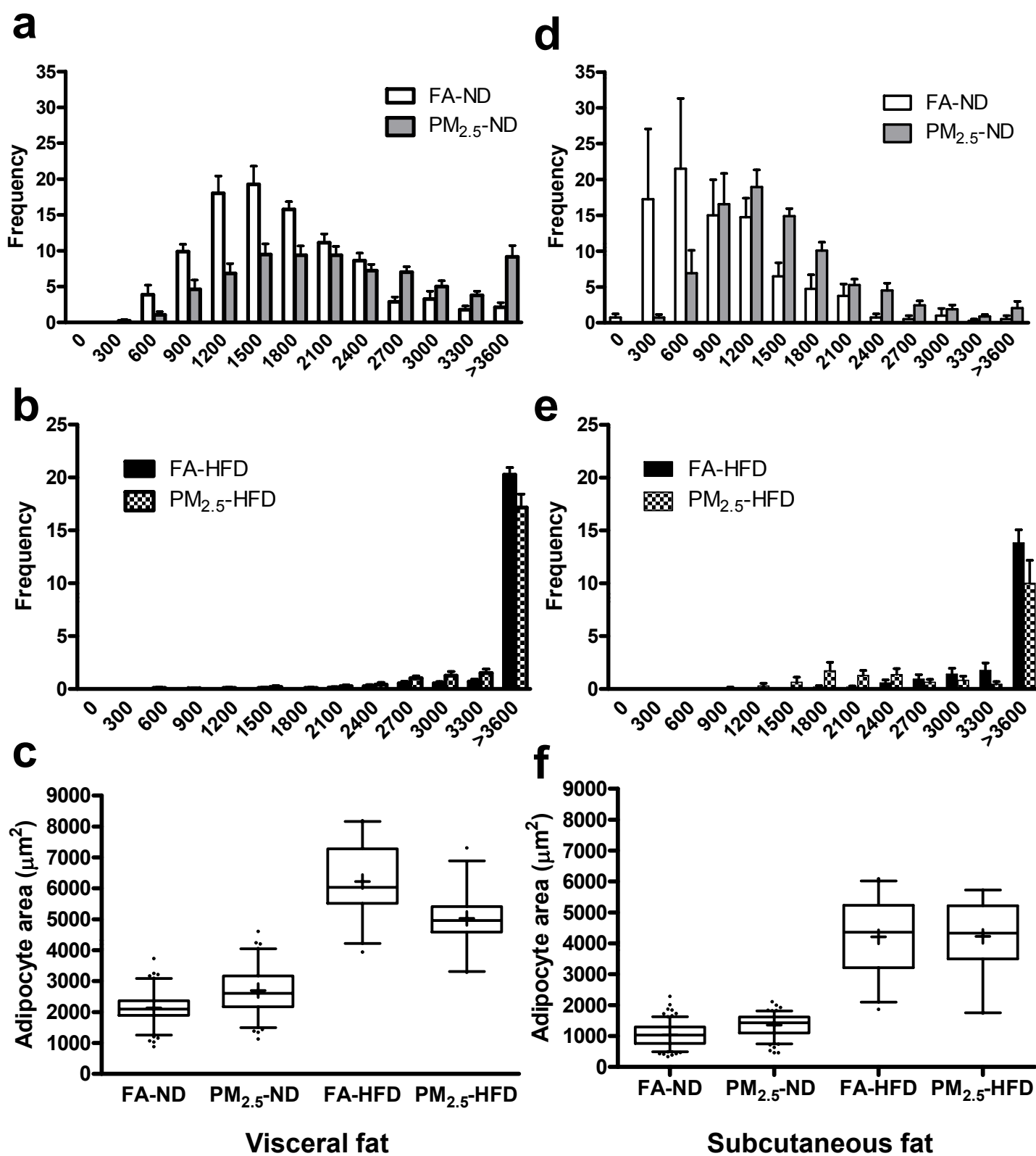
**Supplemental Figure IV.** PM<sub>2.5</sub> exposure induces p47<sup>phox</sup> phosphorylation.

Immunoblots (a) and statistical analysis (b) demonstrated increased p47<sup>phox</sup> phosphorylation in response to PM<sub>2.5</sub> exposure compared to FA in C57BL/6 mice.

Supplemental Figure I

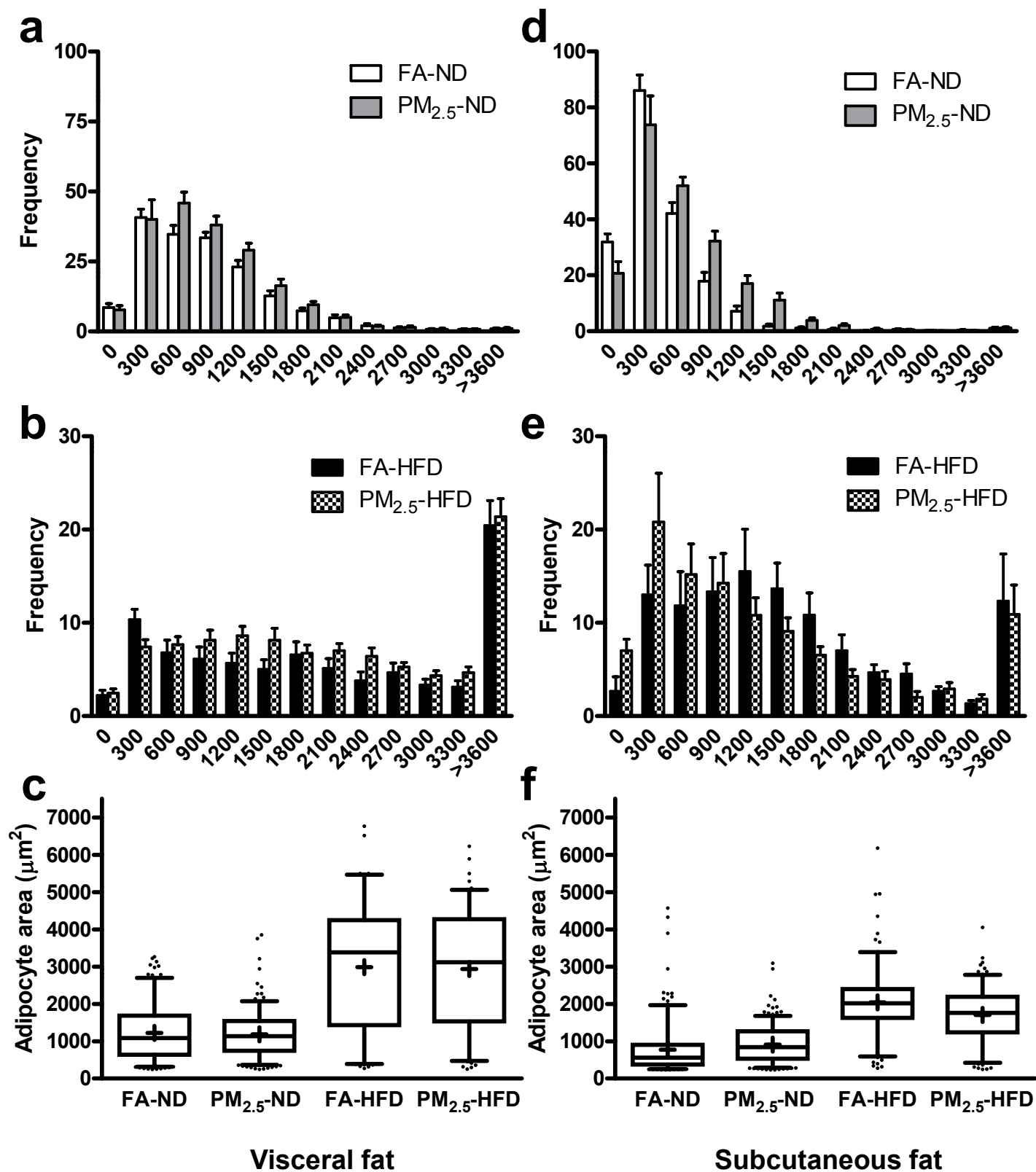


Supplemental Figure II





Supplemental Figure III



Supplemental Figure IV

